

A rhodamine-based fluorescent probe for detecting  $\text{Hg}^{2+}$  in a fully aqueous environment†Cite this: *Dalton Trans.*, 2013, **42**, 14819Xiaoli Chen,<sup>a</sup> Xiangming Meng,<sup>\*a</sup> Shuxing Wang,<sup>a</sup> Yulei Cai,<sup>a,b</sup> Yifan Wu,<sup>a</sup> Yan Feng,<sup>\*a</sup> Manzhou Zhu<sup>a</sup> and Qingxiang Guo<sup>b</sup>

Received 16th May 2013,

Accepted 29th July 2013

DOI: 10.1039/c3dt51279g

www.rsc.org/dalton

A water-soluble fluorescent probe for  $\text{Hg}^{2+}$  based on a rhodamine B derivative was designed and synthesized. The new probe showed reversible colorimetric and fluorescent response to  $\text{Hg}^{2+}$  in a fully aqueous solution. The probe exhibited real-time detection of  $\text{Hg}^{2+}$  with high selectivity in media containing less than 1% organic cosolvent. Furthermore, bioimaging studies indicated that the new probe was cell permeable and suitable for the real-time imaging of  $\text{Hg}^{2+}$  in living cells by confocal microscopy.

## Introduction

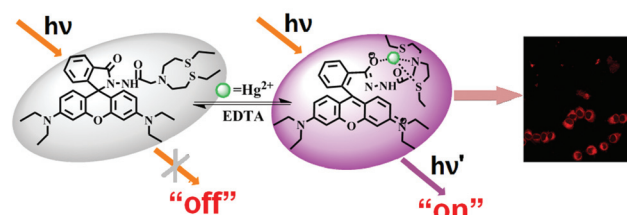
$\text{Hg}^{2+}$  is considered one of the most dangerous and widespread global pollutants, which has a high affinity for thiol groups of proteins and enzymes and causes the dysfunction of the brain, kidney, and central nervous system.<sup>1</sup> On the other hand, mercury ions present in soil or in effluent water can be converted into methylmercury, which will accumulate in organisms and trigger serious disorders in the human body.<sup>2</sup> Therefore, a convenient and rapid method for the determination, especially on-site or in real-time analysis, of mercury in biological and environmental samples is urgent.

Because of the simplicity and high sensitivity of fluorescence, fluorescent probes are regarded as the most powerful tools for monitoring metal ions *in vitro* and/or *in vivo* biologically.<sup>3</sup> A lot of fluorescent probes have been reported.<sup>4</sup> However, turn-on fluorescence probes for  $\text{Hg}^{2+}$  have rarely been reported, due to the fact that  $\text{Hg}^{2+}$  can quench the fluorescence of fluorophores *via* the spin-orbit coupling effect.<sup>5</sup> Among the compounds used as the fluorophores of probes, rhodamine-based dyes have attracted much attention for their excellent spectroscopic properties with large molar extinction coefficients and high fluorescence quantum yields.<sup>6</sup> Furthermore, the spirocyclic forms of rhodamine derivatives are non-fluorescent and colorless, whereas the ring-opening of these derivatives induced by metal ions gives rise to strong

fluorescence emission. This unique structure makes rhodamine dyes good candidates for constructing a “turn-on” fluorescent probe for  $\text{Hg}^{2+}$ .

To date, a lot of rhodamine-based fluorescent probes for  $\text{Hg}^{2+}$  have been reported.<sup>7</sup> However, most of these probes work in organic solvent or water with organic cosolvent,<sup>8</sup> only few of them work well in aqueous buffer solutions containing less than 20% organic cosolvent.<sup>9</sup> This will limit the application of rhodamine-based probes for  $\text{Hg}^{2+}$  detection in biological and environmental systems. To reduce the amount of organic cosolvent during  $\text{Hg}^{2+}$  detection, the structure of rhodamine-based probes needs to be improved to give better water solubility.

Herein, we report a new water soluble rhodamine-based probe (RNS) for  $\text{Hg}^{2+}$  (Scheme 1). This “turn-on” fluorescent probe is composed of two moieties: rhodamine B spirolactam as the potential strong fluorophore and chromophore, and a bis(2-(ethylthio)ethyl)amine ( $\text{NS}_2$ ) fragment as a specific and reversible binding receptor of  $\text{Hg}^{2+}$  due to the thiophilic properties of mercury.<sup>10</sup> For water solubility, a hydrophilic acyl-amino group was used to link the rhodamine B group and the  $\text{NS}_2$  receptor. We speculated that the probe RNS would detect  $\text{Hg}^{2+}$  in water with less or no organic cosolvent.

Scheme 1 The design of RNS for  $\text{Hg}^{2+}$  detection.

<sup>a</sup>Department of Chemistry, Anhui University, Hefei 230039, P. R. China.  
E-mail: mengxm@ahu.edu.cn, fjy70@163.com; Fax: +86-551-5107342;  
Tel: +86-551-5108970

<sup>b</sup>Department of Chemistry, University of Science and Technology, Hefei 230026, P. R. China

†Electronic supplementary information (ESI) available: Photophysical measurements and cell imaging, NMR, crystallographic data. CCDC 938972. For ESI and crystallographic data in CIF or other electronic format see DOI: 10.1039/c3dt51279g

## Experimental

All the reagents were of analytical grade and used as received. All solvents were used after appropriate distillation or purification. All reactions were magnetically stirred and monitored by thin layer chromatography (TLC). Flash chromatography (FC) was performed using silica gel 60 (200–300 mesh). Solutions of  $\text{Hg}^{2+}$ ,  $\text{Fe}^{2+}$ ,  $\text{Na}^+$ ,  $\text{K}^+$ ,  $\text{Mg}^{2+}$ ,  $\text{Mn}^{2+}$ ,  $\text{Fe}^{3+}$ ,  $\text{Cr}^{3+}$ ,  $\text{Co}^{2+}$ ,  $\text{Pb}^{2+}$ ,  $\text{Cu}^{2+}$ ,  $\text{Cd}^{2+}$ ,  $\text{Ni}^{2+}$ ,  $\text{Ca}^{2+}$ ,  $\text{Zn}^{2+}$  and  $\text{Ag}^+$  were prepared from their perchlorate salts.  $^1\text{H}$  and H–H COSY NMR spectra were recorded on Bruker-400 MHz spectrometers and  $^{13}\text{C}$  NMR spectra were recorded on 100 MHz spectrometers. UV-vis spectra were recorded on a Techcomp UV1000 spectrophotometer. Fluorescence responses were recorded on an FL2500 spectrofluorimeter.

### General UV-vis and fluorescence titrations

Inorganic salt was dissolved in distilled water to afford a 10 mM aqueous solution. The 1 mM stock solution of RNS was prepared in absolute methanol. All the measurements were carried out according to the following procedure. To a 10 mL volumetric flask containing 100  $\mu\text{L}$  of the solution of RNS, different amounts (10  $\mu\text{L}$ –500  $\mu\text{L}$ ) of metal ions were added directly with a micropipette, then diluted with buffered (pH 7.0, 20 mM HEPES (4-(2-hydroxyethyl)piperazine-1-erhanesulfonic acid), 50 mM  $\text{NaNO}_3$ ) solution. Fluorescence measurements were carried out with excitation and emission slit widths of 5.0 and 2.5 nm and the PMT voltage and excitation wavelength were 700 V and 520 nm, respectively.

### Synthesis of compound 1

As shown in Scheme 2, compound 1 was prepared according to the literature method.<sup>11</sup>  $^1\text{H}$  NMR ( $\text{CDCl}_3$ , 400 MHz, ppm):  $\delta$ : 1.15 (12H, t,  $J = 7.02$  Hz,  $\text{CH}_3$ ), 3.34 (8H, q,  $J = 7.00$  Hz,  $\text{CH}_2$ ), 3.61 (s, 2H,  $\text{NH}_2$ ), 6.45–6.29 (m, 6H, xanthene-H), 7.10 (m, 1H, Ar-H), 7.45 (m, 2H, Ar-H), 7.93 (m, 1H, Ar-H).  $^{13}\text{C}$  NMR

(DMSO, 100 MHz, ppm),  $\delta$ : 12.4, 43.6, 64.7, 97.4, 105.4, 107.7, 122.1, 123.5, 127.7, 132.4, 148.1, 151.9, 153.0, 165.3.

### Synthesis of compound 2

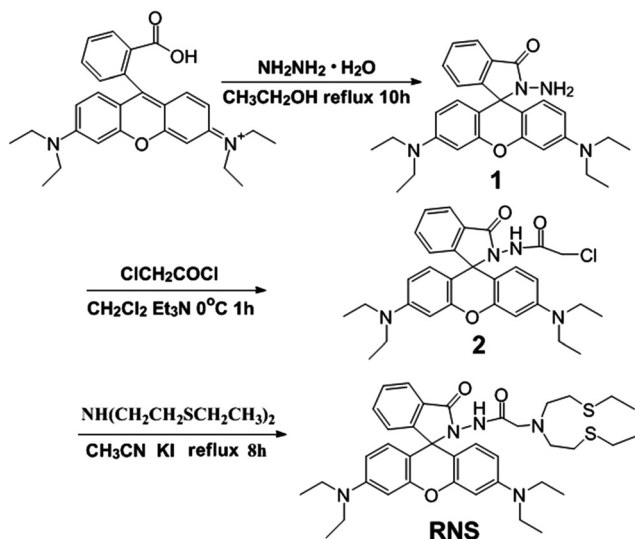
A mixture of compound 1 (1.36 g, 3 mmol), chloroacetyl chloride (0.5 g, 4.5 mmol) and dichloromethane (30 mL) was cooled in an ice bath. Then  $\text{Et}_3\text{N}$  (0.76 g, 7.5 mmol) was dissolved in 5 mL dichloromethane and added dropwise to the solution with vigorous stirring. After the addition, the ice bath was kept for about 30 min, and the color of solution changed from pink to brown. The solvent was removed under reduced pressure to give the crude product. The target product was recrystallized in ethyl acetate to give 1.2 g (75%) of 2.  $^1\text{H}$  NMR (400 MHz, DMSO, ppm),  $\delta$ : 1.17 (12H, t,  $J = 7.03$  Hz,  $\text{CH}_3$ ), 3.34 (8H, q,  $J = 7.02$  Hz,  $\text{CH}_2$ ), 3.61 (2H, s,  $\text{COCH}_2$ ), 6.30 (2H, m, xanthene-H), 6.44 (4H, dd,  $J = 16.14$  Hz, xanthene-H), 7.11 (1H, t,  $J = 8.26$  Hz, Ar-H), 7.45 (2H, m, Ar-H), 7.94 (1H, q,  $J = 5.78$  Hz, Ar-H).  $^{13}\text{C}$  NMR (DMSO, 100 MHz, ppm):  $\delta$ : 12.4, 14.0, 20.7, 40.7, 43.6, 59.7, 65.1, 97.0, 104.0, 107.6, 122.6, 123.8, 128.2, 128.5, 129.1, 133.3, 148.4, 151.8, 153.0, 163.4, 164.6, 170.3.

### Synthesis of compound RNS

A mixture of compound 2 (0.53 g, 1 mmol), bis(2-(ethylthio)ethyl)amine (0.58 g, 3 mmol), KI (0.5 mg, 0.003 mmol) and acetonitrile (20 mL) was heated to 80  $^\circ\text{C}$  for 8 h and cooled to room temperature. Then the reaction mixture was poured into distilled water and extracted by ethyl acetate ( $3 \times 15$  mL). The organic phase was combined, dried over anhydrous  $\text{Na}_2\text{SO}_4$  and concentrated under reduced pressure. The crude product was purified by column chromatography by using the mixed eluent  $\text{EtOAc-PE}$  (1 : 3) to give 0.46 g (67%) of RNS.  $^1\text{H}$  NMR (400 MHz, DMSO, ppm),  $\delta$ : 1.16 (18H, m,  $\text{CH}_3$ ), 2.42 (8H, q,  $J = 7.41$  Hz,  $\text{CH}_2\text{SCH}_2$ ), 2.62 (4H, t,  $J = 7.05$  Hz,  $\text{NCH}_2$ ), 3.12 (2H, s,  $\text{COCH}_2$ ), 3.33 (8H, m,  $\text{NCH}_2\text{CH}_3$ ), 6.29 (2H, d,  $J = 8.69$  Hz, xanthene-H), 6.37 (2H, s, xanthene-H), 6.68 (2H, d,  $J = 8.81$  Hz, xanthene-H), 7.13 (1H, d,  $J = 7.03$  Hz, Ar-H), 7.47 (2H, p,  $J = 7.11$  Hz, Ar-H), 7.94 (1H, d,  $J = 7.35$  Hz, Ar-H), 9.04 (1H, s, NH).  $^{13}\text{C}$ -NMR (DMSO, 100 MHz, ppm),  $\delta$ : 12.6, 14.9, 25.9, 29.4, 44.3, 54.6, 57.9, 65.9, 97.6, 104.4, 107.9, 123.4, 124.0, 128.2, 129.3, 129.4, 132.9, 148.9, 151.7, 153.6, 164.4, 169.1.

### X-ray crystallography

X-ray diffraction data of RNS single crystals were collected on a Siemens Smart 1000 CCD diffractometer. The determination of unit cell parameters and data collection were performed with Mo  $\text{K}\alpha$  radiation ( $\lambda = 0.71073$  Å). Unit cell dimensions were obtained with least-squares refinements, and all structures were solved by direct methods using SHELXS-97.<sup>13</sup> The other non-hydrogen atoms were located in successive difference Fourier synthesis. The final refinement was performed by using full-matrix least-squares methods with anisotropic thermal parameters for non-hydrogen atoms on  $F^2$ . The hydrogen atoms were added theoretically and rode on the concerned atoms. Crystallographic data reported in this



Scheme 2 Synthesis of RNS.

contribution has been deposited with the Cambridge Crystallographic Date Center, CCDC 938972 for RNS (ESI†).

### Cytotoxicity assays

To test the cytotoxic effect of the probe in cells over a 24 h period, an MTT (5-dimethylthiazol-2-yl-2,5-diphenyltetrazolium bromide) assay was performed as previously reported.<sup>12</sup> HeLa cells were passed and plated to *ca.* 70% confluence in 96-well plates 24 h before treatment. Prior to RNS treatment, DMEM (Dulbecco's Modified Eagle Medium) with 10% FCS (Fetal Calf Serum) was removed and replaced with fresh DMEM, and aliquots of RNS stock solutions (5 mM DMSO) were added to obtain final concentrations of 10, 30, and 50  $\mu\text{M}$ . The treated cells were incubated for 24 h at 37 °C under 5%  $\text{CO}_2$ . Subsequently, the cells were treated with 5 mg  $\text{mL}^{-1}$  MTT (40  $\mu\text{L}$  per well) and incubated for an additional 4 h (37 °C, 5%  $\text{CO}_2$ ). Then the cells were dissolved in DMSO (150  $\mu\text{L}$  per well), and the absorbance at 570 nm was recorded. The cell viability (%) was calculated according to the following equation: cell viability % =  $\text{OD}_{570}(\text{sample})/\text{OD}_{570}(\text{control}) \times 100$ , where  $\text{OD}_{570}(\text{sample})$  represents the optical densities of the wells treated with various concentrations of RNS and  $\text{OD}_{570}(\text{control})$  represents that of the wells treated with DMEM plus 10% FCS. The percentage cell survival values are relative to untreated control cells.

## Results and discussion

As shown in Scheme 2, the probe RNS was synthesized *via* four steps from rhodamine B. The structures of RNS and the intermediates were all confirmed by  $^1\text{H-NMR}$  and  $^{13}\text{C-NMR}$  (ESI†). The structure of RNS was also confirmed by X-ray crystallography analysis. The single crystals of RNS grew from anhydrous ether–petroleum ether (60–90 °C) solution. The crystal structure of RNS is depicted in Fig. 1. The parameters associated with the crystal data are shown in Table 1.

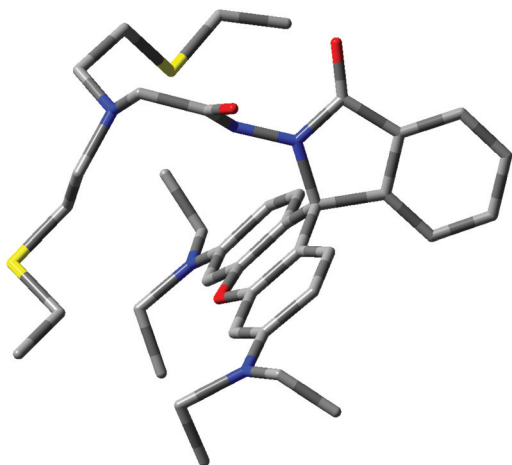


Fig. 1 X-ray crystal structure for RNS. Hydrogen atoms are omitted for clarity.

Table 1 X-ray crystallography data for RNS

Compound reference	RNS
Chemical formula	$\text{C}_{38}\text{H}_{50}\text{N}_5\text{O}_3\text{S}_2$
Formula mass	688.95
Crystal system	Triclinic
Space group	$P\bar{1}$
$a/\text{\AA}$	9.536(5)
$b/\text{\AA}$	11.665(5)
$c/\text{\AA}$	19.178(5)
$\alpha/^\circ$	79.850(5)
$\beta/^\circ$	86.907(5)
$\gamma/^\circ$	67.101(5)
Unit cell volume/ $\text{\AA}^3$	1934.2(14)
Temperature/K	298(2)
$Z$	2
Number of reflections measured	13 975
Number of independent reflections	6888
$R_{\text{int}}$	0.0172
Final $R_1$ values ( $I > 2\sigma(I)$ )	0.0634
Final $wR(F^2)$ values ( $I > 2\sigma(I)$ )	0.2038
Final $R_1$ values (all data)	0.0829
Final $wR(F^2)$ values (all data)	0.2223
Goodness of fit on $F^2$	1.068

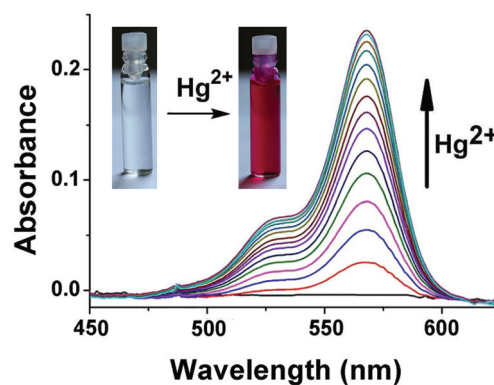
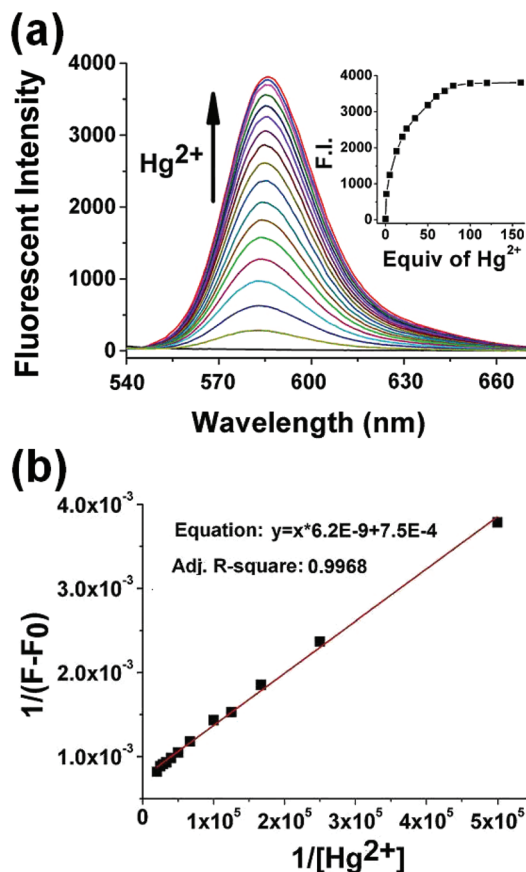


Fig. 2 The UV-vis absorption titration spectra of RNS (10  $\mu\text{M}$ ) with  $\text{Hg}^{2+}$  (0–80 equiv.) in methanol–water (1/99) buffer (pH 7.0, 20 mM HEPES, 50 mM  $\text{NaNO}_3$ ). Inset: digital photographs of RNS and RNS in the presence of an equivalent amount of  $\text{Hg}^{2+}$  under normal light.

### UV-vis and fluorescence spectra responses

The UV-vis titration of RNS with  $\text{Hg}^{2+}$  was carried out in aqueous buffer solution (pH 7.0, 20 mM HEPES, 50 mM  $\text{NaNO}_3$ ). As shown in Fig. 2, the solution of RNS in water was colorless and exhibited no absorption above 500 nm in the UV-vis spectrum, which is ascribed to the spiro-lactam form of RNS. On addition of  $\text{Hg}^{2+}$ , the solution turned from colorless to deep red (Fig. 2, inset). A new and strong absorption centered at 568 nm appeared and was enhanced by the addition of  $\text{Hg}^{2+}$ , suggesting that the formation of the ring-opening of RNS results from  $\text{Hg}^{2+}$  binding. Such a dramatic color change ensures that the RNS can be used as a sensitive “naked-eye” probe for  $\text{Hg}^{2+}$ .

The fluorescent titrations of RNS with  $\text{Hg}^{2+}$  are illustrated in Fig. 3. The free RNS solution showed almost no fluorescent emission. The addition of  $\text{Hg}^{2+}$  caused the intensity of the



**Fig. 3** (a) Fluorescence emission spectra of RNS (10 μM) with excitation at 520 nm, upon titration of Hg<sup>2+</sup> (0–80 equiv.) in methanol–water (1/99) buffer (pH 7.0, 20 mM HEPES, 50 mM NaNO<sub>3</sub>). (b) *B–H* plot (fluorescence at 586 nm) of RNS with Hg<sup>2+</sup> (*F* is the fluorescence intensity of RNS in the presence of Hg<sup>2+</sup> at 586 nm, *F*<sub>0</sub> is the fluorescence intensity of free RNS at 586 nm).

fluorescence at 586 nm to be enhanced dramatically (“turn-on”). When 80 equiv. Hg<sup>2+</sup> was added, the intensity was increased about 1500-fold. The association constant *K*<sub>a</sub> was evaluated using a *B–H* plot.<sup>14</sup> As shown in Fig. 3b, a plot of 1/(*F* – *F*<sub>0</sub>) versus 1/[Hg<sup>2+</sup>] showed a linear relationship, from which one can estimate that RNS was bound with Hg<sup>2+</sup> in a 1 : 1 binding stoichiometry, and the *K*<sub>a</sub> was calculated to be 1.21 × 10<sup>5</sup> M<sup>-1</sup> according to the *B–H* plot. The stoichiometry of the complex of RNS with Hg<sup>2+</sup> was also confirmed by a Job’s plot (Fig. S1, ESI†).

#### Proton NMR spectra

To further elucidate the binding mode, <sup>1</sup>H NMR and H–H COSY experiments were conducted. Fig. 4 shows the RNS’s <sup>1</sup>H NMR change in the absence and presence of Hg<sup>2+</sup> ions. After addition of Hg<sup>2+</sup>, the protons (b, c) beside the S atom displayed apparent downfield shifts of 0.37 and 0.13 ppm, which indicated the coordination of the S atom to Hg<sup>2+</sup>. Protons (d, e) beside the N atom also displayed downfield shifts (Δδ = 0.18, 0.24) resulting from the decrease of the electronic density of the protons, which suggested that Hg<sup>2+</sup> was bound to the N atom of the NS<sub>2</sub> group and the oxygen atom of the carbonyl

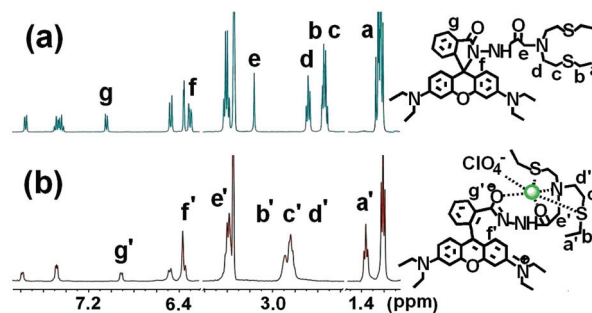


**Fig. 4** The <sup>1</sup>H-NMR spectra of the RNS (a) and RNS + 1 eq. Hg<sup>2+</sup> (b) in CD<sub>3</sub>OD–D<sub>2</sub>O (*v* : *v* = 10 : 1).

group. The proton (g) position showed an upfield shift of 0.14 ppm, which was attributed to the increase in electron density arising from Hg<sup>2+</sup> ion induced opening of the spiro-lactam ring of the RNS. H–H COSY spectra of RNS in the absence and presence of Hg<sup>2+</sup> showed similar results (Fig. S2 and S3, ESI†). Taken together, Hg<sup>2+</sup> was possibly coordinated with the two S atoms and N atom of the receptor, and also with the two oxygen atoms of the carbonyl group of the RNS (Fig. 4).

#### Ion selectivity

Metal ion selectivity studies were performed in HEPES buffer. As shown in Fig. 5a, the addition of Hg<sup>2+</sup> to the solution of RNS induced an obvious fluorescence enhancement. However, other metal ions failed to cause any change of fluorescence of RNS even at higher concentrations. The competitive experiments were carried out in presence of 1.0 equiv. of Hg<sup>2+</sup> mixed with 1.0 equiv. of other transition-metal ions or 50 equiv. of alkali or alkali-earth metal ions in HEPES buffer solutions. Fig. 5b shows that both alkali or alkali-earth metal ions (Na<sup>+</sup>, K<sup>+</sup>, Ca<sup>2+</sup>, Mg<sup>2+</sup>) and transition-metal ions (Cr<sup>3+</sup>, Fe<sup>3+</sup>, Fe<sup>2+</sup>, Cd<sup>2+</sup>, Mn<sup>2+</sup>, Pb<sup>2+</sup>, Zn<sup>2+</sup>, Cu<sup>2+</sup>, Ag<sup>+</sup>, Co<sup>2+</sup>, Ni<sup>2+</sup>) have little effect on the detection of Hg<sup>2+</sup> with RNS. The color change of RNS water solution with different metal ions is shown in Fig. 6. Among the metal ions tested, only Hg<sup>2+</sup> caused dramatic changes both in the color and in fluorescence. Therefore, RNS can serve as a “naked-eye” probe for Hg<sup>2+</sup> with remarkable selectivity in water.

#### pH stability and reversibility test

The effect of pH on the fluorescence emission spectra of free RNS was tested (Fig. 7). The results showed that the solution of RNS was nonfluorescent between pH 6 and 11. However, this solution showed a strong and apparent fluorescence band at 586 nm when the pH value was lower than 6 and increased with a decrease of the solution pH, which signified the spiro-lactam ring opening of RNS because the acyclic forms of rhodamine B derivatives have strong fluorescence around 580 nm. Thus, the pH range of 6–11 is suitable for using RNS for the detection of Hg<sup>2+</sup> ions.

For practical applications, reversibility, the ability to regenerate the free probes from the complex, is also an important parameter for fluorescent probes.<sup>15</sup> To validate the reversibility

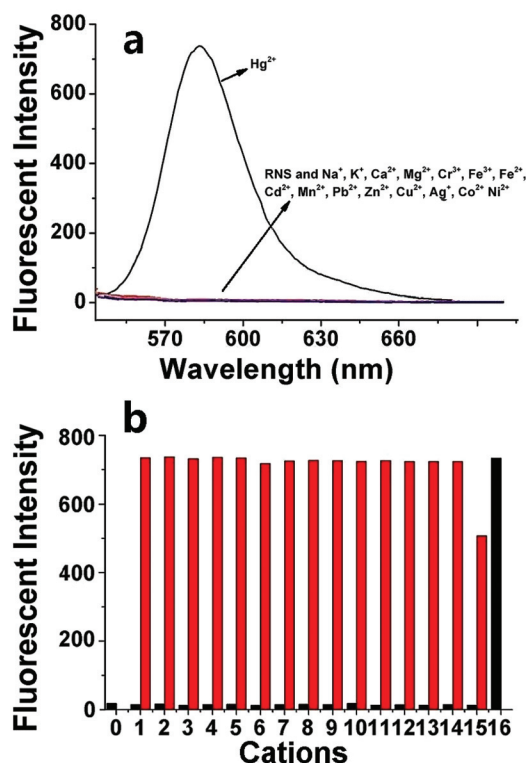


**Fig. 5** (a) Fluorescence spectra of RNS (10  $\mu\text{M}$ ) upon addition of  $\text{Hg}^{2+}$  and other metal ions ( $\lambda_{\text{ex}} = 520 \text{ nm}$ ). (b) Fluorescence intensity at 586 nm of RNS (10  $\mu\text{M}$ ) upon addition of various metal ions (black bars: RNS with other metals, red: RNS with  $\text{Hg}^{2+}$  and other metals). Experimental conditions: methanol–water (1/99) buffer (pH 7.0, 20 mM HEPES, 50 mM  $\text{NaNO}_3$ ), 0.50 mM of  $\text{Na}^+$  (1),  $\text{K}^+$  (2),  $\text{Ca}^{2+}$  (3),  $\text{Mg}^{2+}$  (4); 10  $\mu\text{M}$  of  $\text{Cr}^{3+}$  (5),  $\text{Fe}^{3+}$  (6),  $\text{Fe}^{2+}$  (7),  $\text{Cd}^{2+}$  (8),  $\text{Mn}^{2+}$  (9),  $\text{Pb}^{2+}$  (10),  $\text{Zn}^{2+}$  (11),  $\text{Cu}^{2+}$  (12),  $\text{Ag}^+$  (13),  $\text{Co}^{2+}$  (14),  $\text{Ni}^{2+}$  (15),  $\text{Hg}^{2+}$  (16) ( $\lambda_{\text{ex}} = 520 \text{ nm}$ ).

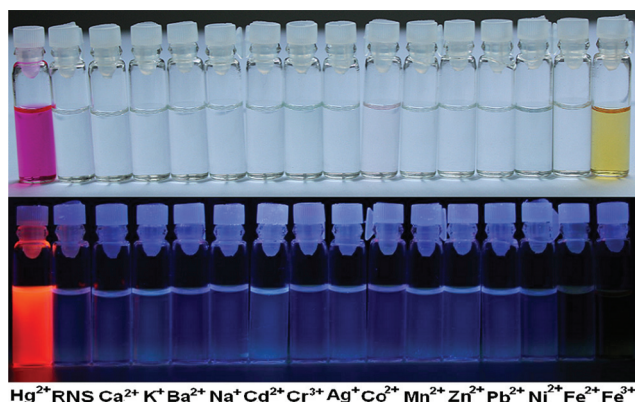


**Fig. 6** Top: color of RNS and RNS with different metal ions. Bottom: fluorescence ( $\lambda_{\text{ex}} = 365 \text{ nm}$ ) change upon addition of different metal ions.

of complexation of RNS and  $\text{Hg}^{2+}$  in a fully aqueous environment, EDTA-addition experiments were performed. When EDTA was added to the solution of the RNS– $\text{Hg}^{2+}$  complex, the fluorescence turned off gradually (Fig. 8). Further addition of excess  $\text{Hg}^{2+}$  could recover the fluorescence of the solution. These results indicated that RNS could serve as a reversible

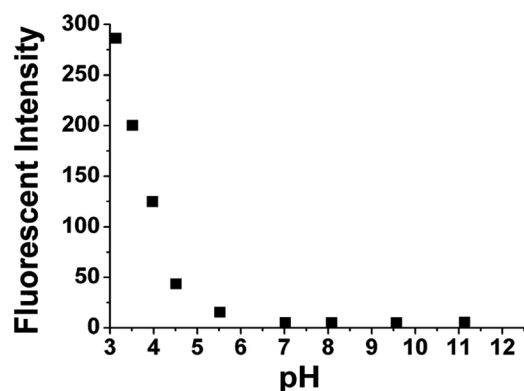


**Fig. 7** Fluorescence of 10  $\mu\text{M}$  RNS at various pH values in methanol–water (1/99) buffer (20 mM HEPES, 50 mM  $\text{NaNO}_3$ ) ( $\lambda_{\text{ex}} = 520 \text{ nm}$ ,  $\lambda_{\text{em}} = 586 \text{ nm}$ ).

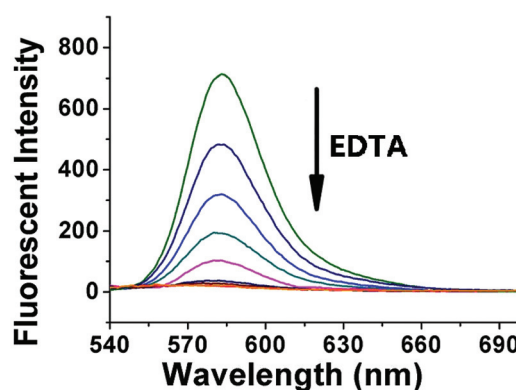


**Fig. 8** The fluorescence titration of EDTA (top to bottom: 0.0, 0.2, 0.4, 0.6, 0.8, 1.0, 1.5 and 2.0 equiv.) in the presence of equimolar RNS/ $\text{Hg}^{2+}$  (10  $\mu\text{M}$ ) in methanol–water (1/99) buffer (pH 7.0, 20 mM HEPES, 50 mM  $\text{NaNO}_3$ ,  $\lambda_{\text{ex}} = 520 \text{ nm}$ ).

probe for  $\text{Hg}^{2+}$  and further confirmed that the fluorescent response of RNS to  $\text{Hg}^{2+}$  was caused by the spiro-ring opening rather than the ion-catalyzed hydrolysis.<sup>16</sup>

Real-time determination is another important factor for a probe for practical application. Time course studies reveal that the recognition response was complete immediately after  $\text{Hg}^{2+}$  addition without any detectable time-delay, which guarantees RNS as a real-time detector for  $\text{Hg}^{2+}$  in water (Fig. S4, ESI<sup>†</sup>).

### Cell imaging

The highly selective real-time response to  $\text{Hg}^{2+}$  makes RNS a probable probe for  $\text{Hg}^{2+}$  imaging in living cells. To confirm this possibility, fluorescence imaging experiments in living cells were carried out. HeLa cells were incubated with a 15  $\mu\text{M}$  solution of the RNS probe for 30 min at 37  $^{\circ}\text{C}$  and then washed with phosphate buffer solution (PBS) to remove excess RNS. As shown in Fig. 9a, no evidence of fluorescence was observed. After further incubation with 30  $\mu\text{M}$   $\text{Hg}(\text{ClO}_4)_2$  for another 2.5 h at 37  $^{\circ}\text{C}$ , a red fluorescence increase was observed from the intracellular region (Fig. 9b). A bright field image of HeLa cells treated with RNS and  $\text{Hg}^{2+}$  confirmed that

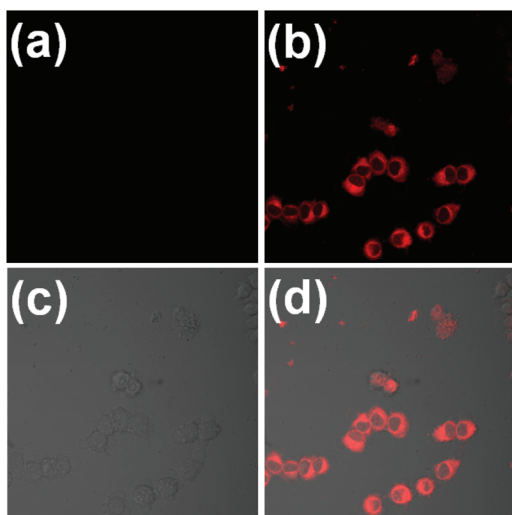


**Fig. 9** Confocal fluorescence, (a) fluorescence image of HeLa cells labeled with 15  $\mu\text{M}$  RNS after 30 min of incubation at 37  $^{\circ}\text{C}$ , washed with PBS buffer. (b) Fluorescence image of HeLa cells treated with RNS and then 30  $\mu\text{M}$   $\text{Hg}(\text{ClO}_4)_2$  aqueous solution for 2.5 h at 37  $^{\circ}\text{C}$ . (c) Bright-field image of HeLa cells. (d) The overlay of (b) and (c).

the cells were viable throughout the imaging experiments (Fig. 9c). Moreover, the MTT assay demonstrates that the cell viability remains more than 95% after treatment with 10  $\mu\text{M}$  RNS after 24 h of incubation (Fig. S5, ESI $^{\dagger}$ ). These results demonstrate that RNS can be used for detecting intracellular  $\text{Hg}^{2+}$  with almost no cytotoxicity.

## Conclusion

In summary, we have developed a fully water soluble rhodamine-based probe (RNS) for  $\text{Hg}^{2+}$  which showed real-time and selective “turn-on” fluorescent response to  $\text{Hg}^{2+}$ . RNS showed reversible colorimetric and fluorescent response to  $\text{Hg}^{2+}$  in an aqueous solution. RNS can work well in neutral aqueous buffer solution containing less than 1% organic cosolvent. Compared with rhodamine-based probes previously reported, the amount of organic cosolvent in the detecting media was greatly reduced. Finally, the confocal fluorescence image confirmed that RNS is cell permeable and can be used for monitoring intracellular  $\text{Hg}^{2+}$  in living cells with low cytotoxicity.

## Acknowledgements

This work was supported by NSFC (21102001, 21102002, 21102083 and 21272223), Natural Science Foundation of Education Department of Anhui Province (KJ2010A028, KJ2011A018), 211 Project of Anhui University, Youth Science Foundation of Anhui University (2009QN014A) and Doctor Research Start-up Fund of Anhui University.

## Notes and references

- (a) B. R. Von, *J. Appl. Toxicol.*, 1995, **15**, 483; (b) G. K. Balendiran, R. Dabur and D. Fraser, *Cell Biochem. Funct.*, 2004, **22**, 343; (c) T. W. Clarkson and L. Magos, *Crit. Rev. Toxicol.*, 2006, **36**, 609; (d) X. M. Meng, L. Liu and Q. X. Guo, *Prog. Chem.*, 2005, **17**, 45.
- (a) T. Takeuchi, N. Morikawa, H. Matsumoto and Y. Shiraishi, *Acta Neuropathol.*, 1962, **2**, 40; (b) W. Y. Boadi, J. Urbach, J. M. Brandes and S. Yannai, *Environ. Res.*, 1992, **57**, 96; (c) M. Harada, *Crit. Rev. Toxicol.*, 1995, **25**, 1; (d) A. C. Bittner Jr., D. Echeverria, J. S. Woods, H. V. Aposhian, C. Naleway, M. D. Martin, R. K. Mahurin, N. J. Heyer and M. Cianciola, *Neurotoxicol. Teratol.*, 1998, **20**, 429.
- (a) J. L. Fan, M. M. Hu, P. Zhan and X. J. Peng, *Chem. Soc. Rev.*, 2013, **42**, 29; (b) X. Q. Chen, G. D. Zhou, X. J. Peng and J. Yoon, *Chem. Soc. Rev.*, 2010, **39**, 2120; (c) Z. C. Xu, J. Yoon and D. R. Spring, *Chem. Soc. Rev.*, 2010, **39**, 1996; (d) Z. P. Liu, W. J. He and Z. J. Guo, *Chem. Soc. Rev.*, 2013, **42**, 1568; (e) L. Yuan, W. Y. Lin, Y. N. Xie, B. Chen and S. Zhu, *J. Am. Chem. Soc.*, 2012, **134**, 1305; (f) C. Streu and E. Meggers, *Angew. Chem., Int. Ed.*, 2006, **45**, 5645; (g) M. Schaferling, *Angew. Chem., Int. Ed.*, 2012, **51**, 3532; (h) F. Qian, C. L. Zhang, Y. M. Zhang, W. J. He, X. Gao, P. Hu and Z. J. Guo, *J. Am. Chem. Soc.*, 2009, **131**, 1460; (i) X. M. Meng, S. X. Wang, Y. M. Li, M. Z. Zhu and Q. X. Guo, *Chem. Commun.*, 2012, **48**, 4196; (j) S. X. Wang, X. M. Meng and M. Z. Zhu, *Tetrahedron Lett.*, 2011, **52**, 2840.
- (a) E. M. Nolan and S. J. Lippard, *Chem. Rev.*, 2008, **108**, 3443; (b) X. M. Meng, L. Liu, H. Y. Hu, M. Z. Zhu and Q. X. Guo, *Tetrahedron Lett.*, 2006, **47**, 7961; (c) A. K. Atta, S. B. Kim, J. Heo and D. G. Cho, *Org. Lett.*, 2013, **15**, 1072; (d) W. M. Xuan, C. Chen, Y. T. Cao, W. H. He, W. Jiang, K. J. Liu and W. Wang, *Chem. Commun.*, 2012, **48**, 7292; (e) W. Y. Lin, X. W. Cao, Y. D. Ding, L. Yuan and L. L. Long, *Chem. Commun.*, 2010, **46**, 3529; (f) S. Yoon, A. E. Albers, A. P. Wong and C. J. Chang, *J. Am. Chem. Soc.*, 2005, **127**, 16030; (g) G. K. Darbha, A. K. Singh, U. S. Rai, E. Yu, H. T. Yu and P. C. Ray, *J. Am. Chem. Soc.*, 2008, **130**, 8038.
- (a) J. R. Lakowicz, *Principles of Fluorescence Spectroscopy*, Springer, New York, 3rd edn, 2006; (b) B. Valeur, *Molecular Fluorescence*, Wiley-VCH, New York, 2nd edn, 2005; (c) X. Q. Chen, T. Pradhan, F. Wang, J. S. Kim and J. Yoon, *Chem. Rev.*, 2012, **112**, 1910; (d) H. N. Kim, W. X. Ren, J. S. Kim and J. Yoon, *Chem. Soc. Rev.*, 2012, **41**, 3210.
- R. P. Haugland, *The Handbook: A Guide to Fluorescent Probes and Labeling Technologies, the Tenth Edition, Molecular Probes*, Invitrogen Corp., Carlsbad, CA, 2005.
- (a) Y. Shiraishi, S. Sumiya, Y. Kohno and T. Hirai, *J. Org. Chem.*, 2008, **73**, 8571; (b) X. Zhang, Y. Xiao and X. H. Qian, *Angew. Chem., Int. Ed.*, 2008, **47**, 8025; (c) M. Kumar, N. Kumar, V. Bhalla, H. Singh, P. R. Sharma and T. Kaur, *Org. Lett.*, 2011, **13**, 1422; (d) Y. K. Yang, K. J. Yook and J. Tae, *J. Am. Chem. Soc.*, 2005, **127**, 16760; (e) P. Mahato, S. Saha, E. Suresh, R. Di Liddo, P. P. Parnigotto,

- M. T. Conconi, M. K. Kesharwani, B. Ganguly and A. Das, *Inorg. Chem.*, 2012, **51**, 1769; (f) H. N. Kim, S.-W. Nam, K. M. K. Swamy, Y. Jin, X. Q. Chen, Y. Kim, S.-J. Kim, S. Park and J. Yoon, *Analyst*, 2011, **136**, 1339; (g) K. M. K. Swamy, H. N. Kim, J. H. Soh, Y. Kim, S.-J. Kim and J. Yoon, *Chem. Commun.*, 2009, 1234.
- 8 (a) Y. Zhou, C.-Y. Zhu, X.-S. Gao, X.-Y. You and C. Yao, *Org. Lett.*, 2010, **12**, 2566; (b) A. Thakur, S. Sardar and S. Ghosh, *Inorg. Chem.*, 2011, **50**, 7066; (c) Q.-B. Mei, Y.-H. Guo, B.-H. Tong, J.-N. Weng, B. Zhang and W. Huang, *Analyst*, 2012, **137**, 5398; (d) M. Suresh, A. K. Mandal, S. Saha, E. Suresh, A. Mandoli, R. Di Liddo, P. P. Parnigotto and A. Das, *Org. Lett.*, 2010, **12**, 5406; (e) R. Pandey, R. K. Gupta, M. Shahid, B. Maiti, A. Misra and D. S. Pandey, *Inorg. Chem.*, 2012, **51**, 298; (f) D. Y. Liu, K. Z. Tang, W. S. Liu, C. Y. Su, X. H. Yan, M. Y. Tan and Y. Tang, *Dalton Trans.*, 2010, **39**, 9763.
- 9 (a) Y. G. Zhao, Z. H. Lin, C. He, H. M. Wu and C. Y. Duan, *Inorg. Chem.*, 2006, **45**, 10013; (b) M.-H. Yang, P. Thirupathi and K.-H. Lee, *Org. Lett.*, 2011, **13**, 5028; (c) M. Santra, B. Roy and K. H. Ahn, *Org. Lett.*, 2011, **13**, 3422.
- 10 (a) J. H. Huang, Y. F. Xu and X. H. Qian, *J. Org. Chem.*, 2009, **74**, 2167; (b) E. M. Nolan and S. J. Lippard, *J. Am. Chem. Soc.*, 2003, **125**, 14270; (c) E. M. Nolan and S. J. Lippard, *J. Am. Chem. Soc.*, 2007, **129**, 5910; (d) Z. Y. Zhang, Y. H. Chen, D. M. Xu, L. Yang and A. F. Liu, *Spectrochim. Acta, Part A*, 2013, **105**, 8.
- 11 (a) X. F. Yang, X. Q. Guo and Y. B. Zhao, *Talanta*, 2002, **57**, 883; (b) L. Jiang, L. Wang, B. Zhang, G. Yin and R. Y. Wang, *Eur. J. Inorg. Chem.*, 2010, 4438; (c) G. M. Fang, Y. M. Li, F. Shen, Y. C. Huang, J. B. Li, Y. Lin, H. K. Cui and L. Liu, *Angew. Chem., Int. Ed.*, 2011, **50**, 7645.
- 12 (a) W. Lin, B. Mohandas, C. P. Fontaine and R. A. Colvin, *BioMetals*, 2006, **20**, 891; (b) Y. M. Li, H. B. Chong, X. M. Meng, S. X. Wang, M. Z. Zhu and Q. X. Guo, *Dalton Trans.*, 2012, **41**, 6189.
- 13 G. M. Sheldrick, *SHELXL-97, Program for refinement of crystal structures*, University of Göttingen, Germany, 1997.
- 14 (a) H. A. Benesi and J. H. Hildebrand, *J. Am. Chem. Soc.*, 1949, **71**, 2703; (b) S. Saha, P. Mahato, G. U. Reddy, E. Suresh, A. Chakrabarty, M. Baidya, S. K. Ghosh and A. Das, *Inorg. Chem.*, 2012, **51**, 336; (c) L. J. Tang, F. F. Li, M. H. Liv and R. Nandhakumar, *Spectrochim. Acta, Part A*, 2011, **78**, 1168; (d) X. Y. Chen, J. Shi, Y. M. Li, F. L. Wang, X. Wu, Q. X. Guo and L. Liu, *Org. Lett.*, 2009, **11**, 4426.
- 15 (a) B. Bag and A. Pal, *Org. Biomol. Chem.*, 2011, **9**, 4467; (b) S. Saha, P. Mahato, M. Baidya, S. K. Ghosh and A. Das, *Chem. Commun.*, 2012, **48**, 9293; (c) E. Coronado, J. R. Galán-Mascarós, C. Martí-Gastaldo, E. Palomares, J. R. Durrant, R. Vilar, M. Gratzel and M. K. Nazeeruddin, *J. Am. Chem. Soc.*, 2005, **127**, 12351.
- 16 (a) J. J. Du, J. L. Fan, X. J. Peng, P. P. Sun, J. Y. Wang, H. L. Li and S. G. Sun, *Org. Lett.*, 2010, **12**, 476; (b) R. Han, X. Yang, D. Zhang, M. Fan, Y. Ye and Y. F. Zhao, *New J. Chem.*, 2012, **36**, 1961; (c) A. B. Rode, J. Kim, S.-H. Kim, G. Gupta and I. S. Hong, *Tetrahedron Lett.*, 2012, **53**, 2571.